An Interpretation of Langmuir Probe Floating Voltage Signals in a Cutting Arc

Leandro Prevosto, Héctor Kelly, and Beatriz Mancinelli

***Abstract*—An experimental study of the electrostatic probe floating voltage signals in a cutting arc and its physical interpretation in terms of the arc plasma structure is reported. Sweeping electrostatic probes have been used to register the local floating potential and ion current at 3.5 mm from the nozzle exit in a 30-A arc generated by a high energy density cutting torch with a nozzle bore radius of 0.5 mm and an oxygen mass flow rate of 0.71 g · s^{-1}. It is found that the floating potential signal presented a central hump with duration almost similar to that corresponding to the ion current signal but having also lateral wings with much larger duration. Capacitive coupling between the probe and the conducting body of the nozzle and arc as a source for the floating potential signal was discarded. It is assumed that the hump in these probe voltage signals results from the presence of an electrostatic field directed in the radial direction outward the arc axis that is caused by thermoelectric effects. The probe floating voltage signal is inverted using the generalized Ohm's law together with the Saha equation, thus obtaining the radial profiles of the temperature, particle densities, radial electric field, and potential of the plasma at the studied section of the arc. The resulting temperature and density profiles derived from our interpretation are in good agreement with the data published elsewhere in this kind of high-pressure arcs. There is not a straightforward connection between the measured hump amplitude in the floating signal (≈4 V) and the derived increase in the plasma potential between the arc edge and the arc center (≈10 V), due to the global zero current balance condition established by the finite size of the probe. It is shown, however, that the probe takes a floating potential value close to that corresponding to the plasma temperature at the probe center.**

***Index Terms*—Cutting torches, Langmuir probes, plasma diagnostic.**

I. Introduction

PLASMA CUTTING torches produce a highly constricted, hot, and high velocity arc plasma jet between a cathode and a workpiece acting as the anode. That plasma is created by a narrow nozzle inside the torch, into which the gas is injected at a high pressure [1]. Although there is a widespread industrial application of this technique, research efforts have appeared more recently in order to understand the main physical processes governing the phenomenon and to develop numerical models for the plasma–gas structure that allows the design of advanced cutting torches.

A classical diagnostic technique that has been employed to study high-pressure arcs is electrostatic (Langmuir) probing. Usually, the floating plasma potential and the ion current are registered with this technique. In these studies, to avoid probe damage, sweeping probes have been employed [2]–[6], usually crossing arc planes that are perpendicular to the current flow direction. The time width of the signals registered in this way can be easily translated into a spatial radial thickness if the probe velocity is known. A characteristic feature of the probe signals in floating conditions is a decrease in the signal amplitude extending outward from the peak center and for some fraction of the peak width. For instance, in Allum's work [3], a 100-A tungsten inert gas (TIG) welding arc was investigated at pressures on the order of or higher than the atmospheric using an electrostatic probe in floating conditions to register the local probe potential in the arc. Their signals showed two distinct regions: an outer zone 20 mm in extent and an inner central zone typically 5 mm wide. Within the central zone, the probe voltage amplitude showed a decrease of about 2 V. Ion saturation current signals were also obtained in this work, and the radial extent of these signals was found to approximately follow that of the central zone identified for floating probe conditions. The author interpreted this result by suggesting that the inner zone corresponded to the current-carrying arc core and the outer zone to a region having a low degree of ionization and essentiality noncurrent-carrying. These regions were also previously identified for high-pressure powerful arcs [7].

In a previous paper [4], an experimental investigation on the arc radial structure in the same kind of high-pressure TIG arc was presented using sweeping probes of different materials in floating conditions. At currents above 50 A, a central decrease in the voltage signal amplitude of the probes in floating conditions was detected, which increased with increasing arc currents at least up to 150 A. A typical peak shape obtained under floating conditions for a 50-A TIG arc showed a reduction in the voltage amplitude of about 1 V. By comparing the signals corresponding to different probe materials, electron thermoionic emission was discarded. No clear explanation of the described signal structure was presented by the authors. No subsequent work has addressed the problem in detail.

Manuscript received August 31, 2008; revised November 13, 2008. First published May 12, 2009; current version published June 10, 2009. This work was supported in part by the University of Buenos Aires (UBA) under Grant PID X111, by the Consejo Nacional de Ciencias y Tecnología (CONICET) under Grant PIP 5378, and by the National Technological University (UTN) under Grant PID UTN Z0007.

L. Prevosto and B. Mancinelli are with the Grupo de Descargas Eléctricas, Departamento Electromecánica, Facultad Regional Venado Tuerto, Universidad Tecnológica Nacional, Venado Tuerto 1347, Argentina, and also with the Instituto de Fisica del Plasma, Consejo Nacional de Investigaciones Científicas y Técnicas, Buenos Aires 1428, Argentina.

H. Kelly is with the Instituto de Fisica del Plasma, Consejo Nacional de Investigaciones Científicas y Técnicas, Buenos Aires 1033, Argentina, and also with the Plasma Physics Laboratory, Departamento de Física, Facultad de Ciencias Exactas y Naturales, University of Buenos Aires, Buenos Aires 1428, Argentina (e-mail: kelly@tinfip.lfp.uba.ar).

Digital Object Identifier 10.1109/TPS.2009.2019277

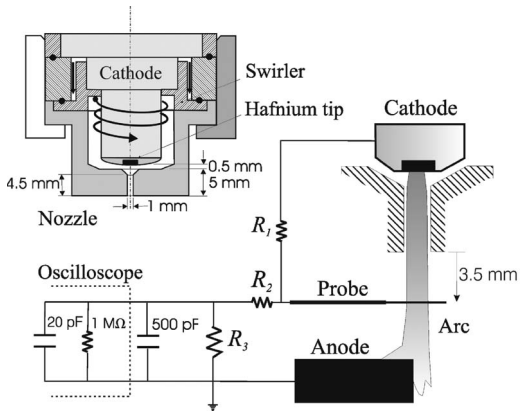

Fig. 1. Schematic of the arc torch, indicating several geometric dimensions. The probe biasing circuit is also shown.

In this paper, an experimental study of electrostatic probe floating voltage signals of the arc generated in a 30-A high energy density cutting torch and its physical interpretation in terms of the arc plasma structure is reported. These torches are characterized by an arc current intensity in the range of 30–100 A, flat cathodes, oxygen as the plasma gas, very small nozzle diameters (≈1 mm), and by the generation of an underexpanded supersonic arc jet with a shock wave close to the nozzle exit [1], [6], [8]–[12]. Using sweeping electrostatic probes, an amplitude reduction in the probe voltage of about 4 V, which is higher than the previously quoted data on welding arcs, is found. It is assumed that the shape of these probe voltage signals results from the presence of a large radial electrostatic field directed outward the arc axis induced by the thermoelectric effect. This effect, which is proportional to the radial electron pressure gradient, becomes quite large due to the arc fineness. Using the generalized Ohm's law together with the Saha equation, the probe floating signal can be inverted to obtain the radial profiles of the temperature, particle densities, radial electric field, and potential of the plasma at a given arc section.

II. Experimental Arrangement

A. Arc Torch

A schematic of the torch indicating several geometric dimensions is shown in Fig. 1. The high energy density cutting torch used in this paper consisted of a cathode centered above an orifice in a converging-straight copper nozzle. The cathode was made of copper (7 mm in diameter) with a hafnium tip (1.5 mm in diameter) inserted at the cathode center. A flow of oxygen gas (mass flow rate of 0.71 $\mathrm{g \cdot s^{-1}}$) cooled the cathode and the nozzle and was also employed as the plasma gas. The gas passed through a swirl ring to provide arc stability. The nozzle consisted in a converging-straight bore (with a converging length of 1 mm and a bore 1 mm in diameter and 4.5 mm in length) in a copper holder surrounding the cathode (with a separation of 0.5 mm between the holder and the cathode surface). To avoid plasma contamination by metal vapors from the anode (usually the workpiece to be cut), a rotating steel disk with 200 mm in diameter and 15 mm in thickness was used as the anode [13]. In this paper, the disk upper surface was located at 5 mm from the nozzle exit. The arc was transferred to the edge of the disk, and the rotating frequency of the disk was equal to 29 Hz. At this velocity, a well-stabilized arc column was obtained, and the lateral surface of the anode disk was completely not melted. Thus, practically no metal vapors from the anode were present in the arc. By machining a small orifice (1 mm in diameter) on the cathode lateral surface, the pressure in the plenum chamber (0.7 MPa) was measured by connecting a pressure meter at the upper head of the cathode.

B. Electrostatic Probe System

The electrostatic probe system employed for studying the arc was similar to that previously reported in [6] and consisted of a thin tungsten wire with a radius $R_p = 0.1$ mm, moving through an arc plane perpendicular to the current flow direction. The probe had a rotary motion (with a constant frequency of 23.8 Hz) on a circumference with a curvature radius of 12 cm. Since this curvature radius is much larger than the arc radius, it can be considered that the probe crosses the arc section with a constant translational velocity $\nu_p = 18\ \mathrm{m \cdot s^{-1}}$. Since a high energy density plasma cutting torch creates an underexpanded sonic flow at the nozzle exit (in our case, photographs of the arc show the presence of a shock wave at $z \approx 1.1$ mm from the nozzle exit, where z is the axial coordinate along the arc), we studied the arc plane at $z = 3.5$ mm. At this axial position, the arc pressure p can be considered to be near the atmospheric value [8].

A schematic of the probe circuit is also shown in Fig. 1. To obtain ion current measurements, the probe was biased with a resistance $(R_1 = 140\ \Omega)$ connected between the probe and the cathode. The ion signal was registered by measuring the voltage on R_1, using a resistive voltage divider ($R_2 = 1\ \mathrm{k\Omega}$ and $R_3 = 12\ \Omega$) with an input resistance value much larger than the R_1 value but with a measuring resistance (R_3) small enough to avoid distortions of the signal due to the discharge of the 500-pF capacitor (corresponding to the measuring coaxial cable) on R_3. This last method of biasing takes advantage of the voltage distribution occurring during the arc discharge, and it was successfully employed in a previous work [6]. To perform probe floating voltage measurements (with respect to the grounded anode) Vf, the values of R_2 and R_3 were changed to $R_2 = 56\ \mathrm{k\Omega}$ and $R_3 = 3.3\ \mathrm{k\Omega}$, while R_1 was disconnected and the voltage on R_3 was registered (see Fig. 1). As it will be shown in the next section, the discharge time of the 500-pF capacitor on the last R_3 value was short enough to avoid signal distortions in floating conditions. The employed oscilloscope was a two-channel Tektronix TDS 1002 B with a sampling rate of 500 MS/s, an analogical bandwidth of 60 MHz, and an input impedance of 1 MΩ in parallel with a stray capacitance of 20 pF.

III. Results

In Fig. 2, typical V_f [Fig. 2(a)] and ion current [Fig. 2(b)] signals are shown. As there is only one probe moving through the arc and the biasing probe circuit to obtain these signals is different, it is impossible to register them simultaneously; thus, its location on the time scale is arbitrary. The reproducibility of these signals was quite good: More than 20 signals of V_f and ion current were registered for the same operating conditions of the torch, and the fluctuations in the amplitude, shape, and

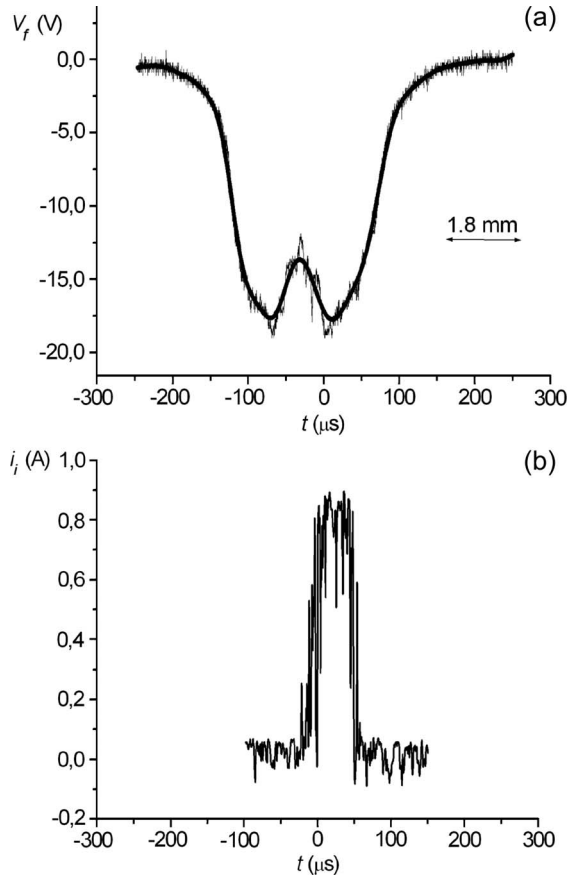

Fig. 2. (a) Typical probe floating signal obtained at 3.5 mm from the nozzle exit. To reduce the noise from the raw data, (thicker line) a fast Fourier transform low-pass filter method was applied. The spatial scale corresponding to the probe velocity is also shown. (b) Typical probe ion current signal.

temporal width of the signals were smaller than 5%. To reduce the noise from the raw data, a fast Fourier transform low-pass filter method was applied on the V_f signal (thicker line). The spatial scale corresponding to the probe velocity is also shown in this figure. Taking into account the resistance value of the voltage divider in floating conditions, the current to the probe $(= V_f/(R_2 + R_3))$ was on the order of 10^{-4} A, which is a value much smaller than that of the ion current [≈1 A; see Fig. 2(b)]. The floating signal [Fig. 2(a)] presents two distinct regions: a central region, with a temporal width of ≈70 μs (which is equivalent to a spatial thickness of ≈1.3 mm, according to the probe speed), where the probe voltage amplitude (always negative) shows a central "hump" with a marked increase of about 4 V toward the arc axis, and a relatively broad outer region, extending ≈150 μs on each side of the central region and corresponding to a total thickness of about 5.5 mm in the spatial scale. As quoted in Section I, the presence of a hump in floating potential signals has been also registered in TIG arcs (see [3, Fig. 3(a) (inset)] and [4, Fig. 3]).

It can be seen by comparing Fig. 2(a) and (b) that the temporal width of the ion current signal (that defines the arc diameter) is quite similar to that corresponding to the central region of V_f. As previously quoted, since the signals correspond to different arc runs, the temporal shift between both signals is meaningless. Based on the similarity between the temporal widths, as well as on the signal reproducibility, we have identified the central hump in the floating voltage signal with the arc diameter, thus defining an "arc radius" R_A of about 0.6–0.7 mm. It will be shown later that the coherent picture that emerges from the analysis of the floating potential signal substantiates the adopted assumption.

To investigate the origin of the outer region in the V_f signal, an additional experiment was arranged: The cathode and the anode were electrically connected using a high resistance (with a value of 30 kΩ), while the nozzle was biased to the cathode using a 50-kΩ rheostat. In this way, and without the presence of the arc, the nozzle was biased to the actual potential when the arc is burning (the nozzle floating voltage), and through the 30-kΩ resistance, a potential distribution very similar to the actual potential distribution was produced. In this situation, the floating voltage induced on a probe passing very close to the torch axis was registered. It was found that this signal had negligible amplitude as compared with that registered with the arc burning [shown in Fig. 2(a)], indicating a negligible capacitive coupling between the probe and the conducting body of the arc and the nozzle. It was then concluded that the outer region of the V_f signal reflects the presence of a weakly ionized region around the arc, which is likely generated by photoionization and electron thermal conduction from the arc core. In this zone, the temperature is insufficient to sustain significant ionization, so that its electrical conductivity σ is negligible compared with that of the arc column.

IV. Interpretation of the Floating Voltage Signals

To obtain a physical interpretation of the hump in the V_f signal shown in Fig. 2(a), we will analyze the fluid electron equation of motion (generalized Ohm's law for a plasma)

$$\overline{E} + \overline{u} \times \overline{B} = \frac{\bar{j}}{\sigma} + \frac{\bar{j} \times \overline{B} - \nabla p_e}{e n_e} \tag{1}$$

where $\overline{E}$ and $\overline{B}$ are the electric and magnetic fields, respectively; $\overline{u}$ is the macroscopic plasma velocity; $\bar{j}$ and n_e are the current and electron density, respectively; e is the electron charge modulus, and p_e is the electron pressure [14]. The second and third terms on the right-hand side of (1) represent the Hall and thermoelectric terms, respectively. Assuming that the plasma is in local thermodynamic equilibrium (LTE), the electron pressure may be expressed as $p_e = n_e kT$, where k and T are the Boltzmann's constant and the plasma temperature, respectively. Although the effects of non-LTE have been studied in cutting torches [11], [12], a theory based on LTE can, in general, make satisfactory temperature predictions when compared with experiments [8]. In cutting arcs, u is on the order of the plasma sound velocity, i.e., on the order of the ion thermal velocity [8], [9], so that $u \approx \sqrt{kT/M}$ (M is the ion mass). The last relation can be used to estimate the magnitude of the third term on the right-hand side of (1), as compared to the term $\overline{u} \times \overline{B}$. Then, it is found that $|\nabla p_e/n_e e|/|\overline{u} \times \overline{B}| \approx kT/(euBR_A) = uM/(eBR_A) = r_{Li}/R_A$, where r_{Li} is the ion Larmor radius. In this problem, it results to $r_{Li}/R_A \gg 1$ because the self-induced $\overline{B}$ is relatively small. A similar estimation can be made between the second and third terms on

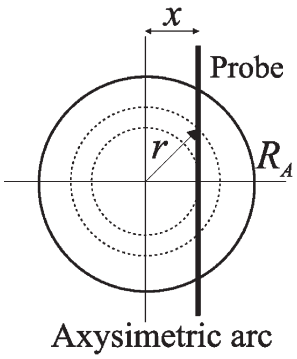

Fig. 3. Schematic of the probe sweeping across the plasma at a generic time.

the right-hand side of (1), so that it can be written as $|\nabla p_e|/|\bar{j} \times \overline{B}| \approx (kn_eT/R_A)/(\mu_0 I^2/4\pi^2 R_A^3)$. For typical values of the plasma quantities of a 30-A cutting torch at the arc axis and close to the nozzle exit, $T \approx 1.5 \times 10^4$ K and $n_e \approx 10^{23}$ m^{-3} [8], [15], it results to $|\nabla p_e|/|\bar{j} \times \overline{B}| \approx 10^2 \gg 1$. With the described simplifications, the Ohm's law becomes

$$\overline{E} + \frac{1}{en_e}\nabla p_e = \frac{\bar{j}}{\sigma}. \tag{2}$$

The radial component of (2) can be written as

$$E_r + \frac{k}{en_e}\left(n_e\frac{\partial T}{\partial r} + T\frac{\partial n_e}{\partial r}\right) = \frac{j_r}{\sigma} = 0 \tag{3}$$

where r is the radial coordinate. The last equality in (3) follows from the fact that the electric current is almost directed in the z-direction ($j_z \gg j_r$). In highly constricted arcs, the radial thermoelectric term can reach high values (on the order of 10^4 V $\cdot$ m^{-1}; see Fig. 6 later), which means that it is even larger than the main (axial) electric field in the arc column [15]. Therefore, a high electrostatic radial field is induced in order to balance the thermoelectric term in the radial direction. Using the relationship $E_r = -\partial V_s/\partial r$, where V_s is the electrostatic plasma potential, (3) can be written as

$$\frac{\partial V_s}{\partial r} = \frac{k}{en_e}\left(n_e\frac{\partial T}{\partial r} + T\frac{\partial n_e}{\partial r}\right). \tag{4}$$

A geometrical sketch of the probe passing through the arc section at a generic time t is shown in Fig. 3. Since the probe side length is large as compared with the arc diameter, each differential length element of the probe will collect charges from a small plasma volume with different plasma quantity values (T and n_e). Since the probe is an equipotential, this means that, in floating conditions (when the current to the probe is approximately zero), the zero current balance will be fulfilled not locally but globally. Some elements of the probe will collect a net electron current i_e, while other elements will collect a net ion current i_i, to yield a total resultant current $i_p \equiv i_e - i_i = 0$.

Assuming a circular symmetry for the arc section, the arc core can be divided into several concentric elemental rings, so that the probe current can be expressed as the sum of contributions from many regions with different plasma quantity and potential values, but at the same probe potential $V_f(x)$, where x is the coordinate of the probe axis. As the electron thermal velocity $\overline{\nu}_e \equiv \sqrt{8kT/(\pi m)}$ (m is the electron mass) is very large compared to the fluid-plasma velocity, the usual expression for the electron current collected by a probe in high-pressure quiescent plasmas applies. Under floating conditions, this electron current (per-unit probe length) for a cylindrical probe is given from the expression presented in [16] but replacing the generic probe potential by its floating value $V_f(x)$

$$i'_e = 2\pi R_p \frac{1}{\gamma}\frac{en_e\overline{\nu}_e}{4}\exp\left(-\frac{e\,|V_f(x) - V_s(r)|}{kT}\right) \tag{5}$$

where the correction factor γ is given by [16] $\gamma \approx 1 + (\lambda_D/2\lambda_{ea})(kT/e(V_f - V_s))$, where λ_D is the electron Debye length and λ_{ea} the electron mean free path for collisions with neutrals. The factor γ is very close to unity in the temperature range of interest 5000 K–15 000 K ($\lambda_D \ll \lambda_{ea}$, and $kT/e < |V_f - V_s|$), and therefore, $\gamma = 1$ was taken. The ion current (per-unit length probe) under floating conditions for a cylindrical probe in a high-pressure high-velocity plasma jet is given from the expression presented in [15] but replacing the generic probe potential by its floating value $V_f(x)$

$$i'_i = 0.46\, en_i\nu_B\lambda_{ia}\frac{e\,|V_f(x) - V_s(r)|}{kT} \tag{6}$$

where n_i is the ion density, $\nu_B \equiv \sqrt{kT/M}$ is the Bohm velocity, and λ_{ia} is the ion mean free path for collisions between ions and neutrals, defined as $\lambda_{ia} \equiv 1/n_n\sigma_0$, where n_n is the neutral density and σ_0 is the elastic cross section, which is typically $\approx 5 \times 10^{-19}$ m^2 [17].

Taking into account (5) and (6), and using simple geometrical considerations, one can write the total current ($= 0$) to the probe under floating conditions in terms of an integral along the radial direction as follows:

$$i_p(x \equiv \nu_p t) = 2 \times \int_{r=|x|}^{R_A} i'_e \frac{r}{\sqrt{r^2 - x^2}}\,dr - 2 \times \int_{r=|x|}^{R_A} i'_i \frac{r}{\sqrt{r^2 - x^2}}\,dr = 0. \tag{7}$$

Other equations that can be used are the Saha equation

$$\frac{n_e n_i}{n_n} = 2\frac{Q_i}{Q_n}\left(\frac{2\pi mkT}{h^2}\right)^{3/2}\exp\left(-\frac{E_I}{kT}\right) \tag{8}$$

and the equation of state

$$p = (n_e + n_i + n_n)kT \tag{9}$$

where Q_i and Q_n are the statistical weights of oxygen ions and atoms, respectively; E_I is the oxygen ionization energy; and h is the Planck's constant. Neglecting radial oscillations of the arc during the crossing time of the probe, the plasma pressure can be considered as a constant along the arc section.

The plasma is assumed to be electrically neutral and the density of doubly ionized ions is considered to be negligible, so that

$$n_e = n_i \equiv n. \tag{10}$$

If the plasma pressure is known, (4), (7)–(10), together with the experimental registered data for V_f, represent a closed system to obtain the five unknown quantities of the problem: n_e,

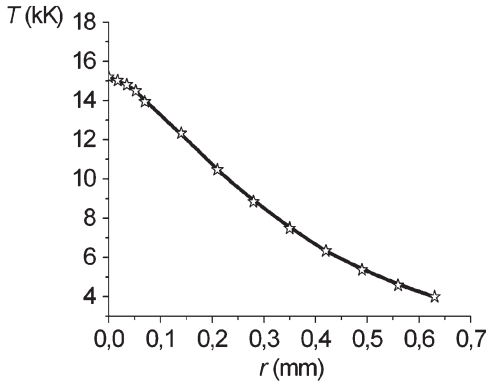

Fig. 4. Radial profile of the plasma temperature obtained at 3.5 mm from the nozzle exit.

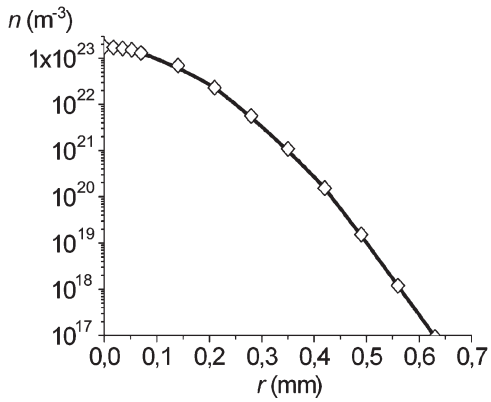

Fig. 5. Radial profile of the plasma density obtained at 3.5 mm from the nozzle exit.

n_i, n_n, T, and V_s. We have considered in this case a pressure value of 0.13 MPa for an arc section located at 3.5 mm from the nozzle exit. Note that an overpressure value of 0.03 MPa was included to take into account the stagnation effects at the upstream edge of the probe surface for a plasma flow velocity of $\approx 2 \times 10^3$ m $\cdot$ s^{-1} (on the order of the ion sound velocity) and a plasma density corresponding to a pressure of 0.1 MPa and a temperature of 15 000 K (as it will be shown later, this is a typical value obtained for T).

To solve the system of equations, the arc core was subdivided into N differential concentric rings. In order to obtain a good behavior for the solutions close to the arc axis, the thicknesses of the rings were reduced in this region. In practice, it was found that $N = 13$ was high enough to obtain smooth radial profiles of the unknowns. Similar values of N have been successfully used in inversions of physical quantities having its maximum values at the center of the distribution [18]. Since (4) is a first-order differential equation, it is necessary to know a boundary value of one quantity for obtaining the solution. Taking into account the particular coupling of the quantities in the equation system, we have chosen to give the plasma temperature at the arc outer border [$T(R_A)$] as the prescribed boundary condition.

Replacing (4), (8)–(10) into (7), this last equation becomes an integral function of $T(r)$ and $V_f(x)$. Note that, for a given value of x (with a corresponding value of $V_f(x)$ obtained from the experimental signal), (7) allows one to obtain a temperature radial profile within the range $|x| < r < R_A$ [this range comes from the integral limits in (7)]. Thus, the complete temperature radial profile can be obtained, starting with $x = R_A$ and therefore taking lower x values until reaching the arc center.

In practice, to invert this equation, a discretization of the integral into a set of N linear equations was performed, allowing one to obtain the T^i value in terms of the previously obtained T^{i+1} value ($i = 1, 2, \ldots, N$). Using the obtained T profile, the rest of the plasma quantities can be derived.

In Fig. 4, the predicted $T(r)$ profile is presented for $T(R_A) = 4000$ K. As can be seen, the temperature profile shows a peak value of about 15 000 K at the arc center and decreases monotonically to the arc edge. The $n(r)$ profile is shown in Fig. 5. As expected, the larger plasma density values are concentrated in the region of high temperature values ($T >$ 10 000 K) with an axial peak density value of about 10^{23} m^{-3}. These results are in good agreement with previously published

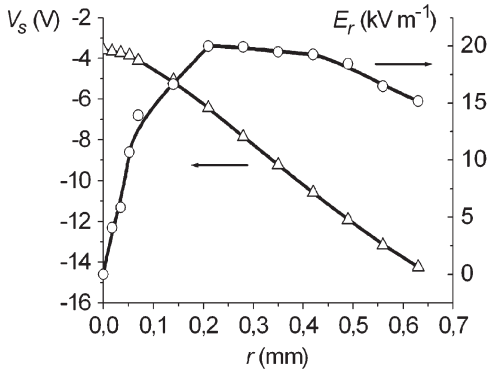

Fig. 6. Radial profiles of the radial electric field and plasma potential obtained at 3.5 mm from the nozzle exit.

results [15] obtained using ion current measurements from electrostatic probes at the same axial position of the arc investigated in this paper. Moreover, a numerical simulation of a similar 30-A oxygen arc cutting torch (validated with spectroscopic temperature measurements) [8] predicts temperature profiles close to those obtained here. In Fig. 6, the resulting electrostatic field and plasma potential radial profiles are shown. As can be seen, the radial electric field value is high, which is up to 20 V $\cdot$ mm^{-1}, being even higher than the axial electric field values in the external part of the arc $\approx$7 V $\cdot$ mm^{-1} [15]. The $V_s(r)$ curve presents a marked decrease toward the arc axis (of about 10 V) produced by the strong electric field.

It must be noted that the selected value for $T(R_A) = 4000$ K was guided by the $\sigma(T)$ behavior for a 0.1-MPa oxygen gas, with σ being very small for T in the range 4000 K–5000 K and then growing steeply as the temperature increases [16], [19]. Since the final solution is quite sensitive to the $T(R_A)$ value, its final value was chosen to obtain a T value at the arc center similar to the other published values [8], [15].

It must be noted that there is not a straightforward connection between the measured hump amplitude in the floating signal ($\approx$4 V) and the derived increase in the plasma potential between the arc edge and the arc center ($\approx$10 V), due to the global zero current balance condition established by the finite size of the probe. Taking into account that the electron current to a probe is much larger than the corresponding ion current for a given absolute value of the potential drop between probe and plasma, it is clear that a probe crossing the arc at a generic position (see

Fig. 3) will take a floating potential close to that corresponding at the probe center, because at this point, the plasma temperature is the largest and, otherwise, the zero current balance will never be satisfied. This point can be quantitatively confirmed by deriving an "effective plasma temperature" (T^*) from a simple formula (corresponding to a homogeneous plasma) relating the experimental floating potential [shown in Fig. 2(a)] and the derived plasma potential (shown in Fig. 6) with T^*. By equating (5) and (6), it is found that T^* remains close but a little higher than the plasma temperature at the probe center, with a maximum difference between both temperatures of about 2000 K at the arc center. If, to a first approximation, one considers that the probe takes a floating potential value corresponding to the arc temperature at its center, in the case of TIG arcs, the smaller measured hump amplitude in the floating signal ($\approx$1 or 2 V, according to the arc current) can be attributed to a temperature profile with smaller values [1], [2] than that commonly found with cutting torches.

V. Final Remarks

In this paper, an experimental study of the electrostatic probe floating voltage signals in a cutting arc and its physical interpretation in terms of the arc plasma structure has been reported. Sweeping electrostatic probes have been used to register the local floating potential and ion current at 3.5 mm from the nozzle exit in a 30-A arc generated by a high energy density cutting torch with a nozzle bore radius of 0.5 mm and an oxygen mass flow rate of 0.71 $\mathrm{g \cdot s^{-1}}$. It was found that the floating potential signals presented a central hump with duration almost similar to that corresponding to the ion current signal but having also lateral "wings" with much larger duration. A special experiment arranged to simulate a voltage distribution without the arc similar to the actual voltage distribution with the arc running allowed one to discard capacitive coupling between the probe and the conducting body of the nozzle and arc as a source for the floating potential signal. The measurements showed an amplitude reduction in the floating voltage hump of about 4 V, which is higher than other reported data in thicker welding arcs.

It was assumed that the hump in these probe voltage signals results from the presence of an electrostatic field directed in the radial direction outward the arc axis that is caused by thermoelectric effects. Using the generalized Ohm's law together with the Saha equation, it was possible to invert the probe floating voltage signal, thus obtaining the radial profiles of the temperature, particle densities, radial electric field, and potential of the plasma at the studied section of the arc. The resulting $T(r)$ and $n(r)$ profiles derived from our interpretation are in good agreement with data published elsewhere [8], [15] in this kind of high-pressure arcs.

There is not a straightforward connection between the measured hump amplitude in the floating signal ($\approx$4 V) and the derived increase in the plasma potential between the arc edge and the arc center ($\approx$10 V), due to the global zero current balance condition established by the finite size of the probe. It was shown, however, that the probe takes a floating potential value close to that corresponding to the plasma temperature at the probe center.

References

[1] V. A. Nemchinsky and W. S. Severance, "What we know and what we do not know about plasma arc cutting," *J. Phys. D, Appl. Phys.*, vol. 39, no. 22, pp. R423–R438, Nov. 2006.

[2] A. E. F. Gick, M. B. C. Quigley, and P. H. Richards, "The use of electrostatic probes to measure the temperature profile of welding arcs," *J. Phys. D, Appl. Phys.*, vol. 6, no. 16, pp. 1941–1949, Oct. 1973.

[3] C. J. Allum, "Power dissipation in the column of a TIG welding arc," *J. Phys. D, Appl. Phys.*, vol. 16, no. 11, pp. 2149–2165, Nov. 1983.

[4] C. Fanara and I. M. Richardson, "A Langmuir multi-probe system for the characterization of atmospheric pressure arc plasmas," *J. Phys. D, Appl. Phys.*, vol. 34, no. 18, pp. 2715–2725, Sep. 2001.

[5] C. Fanara, "Sweeping electrostatic probes in atmospheric pressure arc plasmas—Part I: General observations and characteristic curves," *IEEE Trans. Plasma Sci.*, vol. 33, no. 3, pp. 1072–1081, Jun. 2005.

[6] L. Prevosto, H. Kelly, and B. Mancinelli, "On the use of sweeping Langmuir probes in cutting arc plasmas—Part I: Experimental results," *IEEE Trans. Plasma Sci.*, vol. 36, no. 1, pp. 263–270, Feb. 2008.

[7] G. R. Jones and M. T. C. Fang, "The physics of high-power arcs," *Rep. Prog. Phys.*, vol. 43, no. 12, pp. 1415–1465, Dec. 1980.

[8] P. Freton, J. J. Gonzalez, A. Gleizes, F. Camy Peyret, G. Caillibotte, and M. Delzenne, "Numerical and experimental study of a plasma cutting torch," *J. Phys. D, Appl. Phys.*, vol. 35, no. 2, pp. 115–131, Jan. 2002.

[9] P. Freton, J. J. Gonzalez, F. Camy Peyret, and A. Gleizes, "Complementary experimental and theoretical approach to the determination of the plasma characteristics in a cutting plasma torch," *J. Phys. D, Appl. Phys.*, vol. 36, no. 11, pp. 1269–1283, Jun. 2003.

[10] L. Girard, P. Teulet, M. Razafinimanana, A. Gleizes, F. Camy-Peyret, E. Baillot, and F. Richard, "Experimental study of an oxygen plasma torch: I. Spectroscopic analysis of the plasma jet," *J. Phys. D, Appl. Phys.*, vol. 39, no. 8, pp. 1543–1556, Apr. 2006.

[11] S. Ghorui, J. V. R. Heberlein, and E. Pfender, "Non-equilibrium modeling for an oxygen plasma cutting torch," *J. Phys. D, Appl. Phys.*, vol. 40, no. 7, pp. 1966–1976, Apr. 2007.

[12] J. Peters, J. Heberlein, and J. Lindsay, "Spectroscopic diagnostics in a highly constricted oxygen arc," *J. Phys. D, Appl. Phys.*, vol. 40, no. 13, pp. 3960–3971, Jul. 2007.

[13] S. Ramakrishnan, M. Gershenzon, F. Polivka, T. N. Kearny, and M. W. Rogozinsky, "Plasma generation for the plasma cutting process," *IEEE Trans. Plasma Sci.*, vol. 25, no. 5, pp. 937–946, Oct. 1997.

[14] R. J. Goldston and P. H. Rutherford, *Introduction to Plasma Physics*. Bristol, U.K.: Inst. Phys. Publishing, IOP, 1995.

[15] L. Prevosto, H. Kelly, and F. Minotti, "On the use of sweeping Langmuir probes in cutting arc plasmas—Part II: Interpretation of the results," *IEEE Trans. Plasma Sci.*, vol. 36, no. 1, pp. 271–277, Feb. 2008.

[16] Y. P. Raizer, *Gas Discharge Physics*. Berlin, Germany: Springer-Verlag, 1991.

[17] H. L. Anderson, *A Physicist's Desk Reference*, 2nd ed. New York: AIP, 1989.

[18] W. Lochte-Holtgreven, *Plasma Diagnostics*. New York: AIP Press, 1995, ch. 3.

[19] M. Boulos, P. Fauchais, and E. Pfender, *Thermal Plasmas, Fundamentals and Applications*, vol. 1. New York: Plenum, 1994.

Leandro Prevosto was born in Santa Fe, Argentina, on November 29, 1971. He received the Engineer degree in electromechanical engineering from the Universidad Tecnológica Nacional, Venado Tuerto, Argentina, in 2005. He is currently working toward the Ph.D. degree in the Instituto de Física del Plasma, Consejo Nacional de Investigaciones Científicas y Técnicas, Buenos Aires, in the Grupo de Descargas Eléctricas, Departamento Electromecánica, Facultad Regional Venado Tuerto, Universidad Tecnológica Nacional, and in the Facultad de Ingeniería, Universidad de Buenos Aires, under a fellowship from the Fundación Yacimientos Petrolíferos Fiscales, Argentina.

Héctor Kelly was born in Mendoza, Argentina, on February 14, 1948. He received the M.S. and Ph.D. degrees in physics from the University of Buenos Aires, Buenos Aires, Argentina, in 1972 and 1979, respectively.

He has been a Researcher with the Plasma Physics Laboratory, Departamento de Física, Facultad de Ciencias Exactas y Naturales, University of Buenos Aires, since 1973 and the Instituto de Fisica del Plasma, Consejo Nacional de Investigaciones Científicas y Técnicas, Buenos Aires, since 1980. His current research interests are high power electric discharges, vacuum arcs, and nonthermal high-pressure plasmas.

Beatriz Mancinelli was born in Santa Fe, Argentina, on February 6, 1965. She received the Engineer degree in nuclear engineering from the Instituto Balseiro, San Carlos de Bariloche, Argentina, in 1990. She is currently working toward the Ph.D. degree in the Instituto de Física del Plasma, Consejo Nacional de Investigaciones Científicas y Técnicas, Buenos Aires, in the Grupo de Descargas Eléctricas, Departamento Electromecánica, Facultad Regional Venado Tuerto, Universidad Tecnológica Nacional, and in the Facultad Regional Córdoba, Universidad Tecnológica Nacional, under a fellowship from the Universidad Tecnológica Nacional.